Time Domain Optimization of Voltage and Current THD for a Three-Phase Cascaded H-Bridge Inverter

Rassul Bairamkulov and Alex Ruderman
Department of Electrical and Electronic Engineering
Nazarbayev University
Astana, 010000 Kazakhstan
{rbairamkulov & alexander.ruderman}@nu.edu.kz

Yakov L. Familiant
Department of Robotics and Mechatronics
Nazarbayev University
Astana, 010000 Kazakhstan
yakov.familiant@nu.edu.kz

***Abstract*–This paper addresses optimal voltage and current quality in the sense of minimal Total Harmonic Distortion (THD) for a three-phase cascaded H-bridge inverter with a fundamental switching staircase modulation. THD minimization problems are formulated in time domain as constraint optimization ones in order to find theoretically optimal switching angles accounting for all switching harmonics. Provided are numerically obtained optimal switching angles and minimal voltage and current THD values for the overall output voltage dynamic range for a basic converter with two H-bridge modules per phase. While optimal three-phase inverter voltage THD solutions were already reported in literature, optimal current THD ones are supposed to be systematically presented for the first time.**

***Keywords*–Multilevel Inverter, Cascaded H-Bridge, Staircase Modulation, Optimal Switching Angles**

I. INTRODUCTION

Multilevel inverters are being widely used for medium / high voltage and other applications [1]-[3]. Over the past years, power electronics research community has shown significant interest in voltage and current THD analysis for multilevel PWM and optimization for multilevel staircase modulation. Every year there are about 100 multilevel inverter papers that end up with voltage and / or current THD evaluation results that are typically based on frequency spectra numerical calculations or measurements.

Analytical solutions for voltage THD of multilevel PWM single- and three-phase inverters were obtained in [4] in asymptotic approximation (high switching-to-fundamental frequency ratio).

Assuming pure inductive load, current THD actually becomes frequency Weighted voltage THD (WTHD). This approximation is practically accurate for inductance dominated RL-loads meaning that the load time constant is much larger than switching intervals. Asymptotic current THD for a single-phase multilevel PWM inverter recently reported in [5] employs current ripple approximation by time integration of the voltage one that originates to [6].

For fundamental frequency switching, much work has been done on Selective Harmonics Elimination (SHE) techniques [7]. However, while SHE can totally eliminate certain low order harmonics, it was recognized that it does not minimize voltage / current THD. Also SHE solutions typically exist for a limited fundamental harmonic (modulation index) interval.

Many multilevel inverter researchers use a limited harmonics count (51 as recommended by IEEE Standard 519 [8] or other like 101) to evaluate multilevel voltage / current quality that may cause a THD underestimation.

There is a widely spread misconception that it is impossible to account for the infinite harmonics count while making an evaluation of multilevel inverter voltage and current quality. In fact, it is possible that was recently demonstrated for a single-phase inverter voltage THD by making squared multilevel voltage waveform time averaging ([9]-[11]). This approach combined with constrained optimization was systematically applied to a multilevel single-phase inverter voltage and current THD minimization in [12].

So far, while considering three-phase cascaded H-bridge inverters, the researchers employed conventional frequency domain THD definition that resulted in THD underestimation [13]-[16]. Current THD is typically addressed as frequency Weighted THD (WTHD) [15].

In [17], the authors account for all switching harmonics by finding closed form expressions for infinite sums that appear in THD frequency domain definition. This approach requires high math skills and much effort is spent on tedious calculations instead of focusing on the physical essence of the problem. This extra effort may be totally eliminated by applying time domain analysis as it is done in this paper. While presented below voltage THD results are practically identical to those of [17], current THD optimal switching angles and minimal current THD are believed to be presented for the first time.

II. SINGLE-PHASE INVERTER MINIMAL VOLTAGE AND CURRENT THD TIME DOMAIN PROBLEM FORMULATION

Fig.1 presents elementary staircase voltage waveform with two independent switching angles that is due to quarter-wave symmetry.

By frequency domain definition, voltage THD expression

$$THD(m),\% = \frac{\sqrt{\sum_{n\neq 1}^{\infty} V_n^2}}{V_1}. \quad (1)$$

An accurate closed-form expression for a voltage waveform approximation error Normalized Mean Square (voltage ripple NMS [5], [12]) is obtained by calculating squared (normalized) voltage waveform average on a quarter-wave time interval as

$$NMS(m) = \frac{2}{\pi}\int_0^{\pi/2} v^2(\tau)d\tau - \frac{1}{2}m^2. \quad (2)$$

978-1-5090-1798-0/16/$31.00 ©2016 IEEE

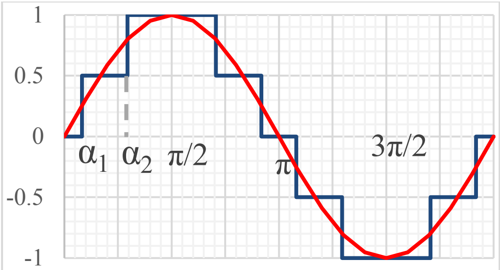

Fig. 1. Three-level single-phase inverter voltage waveform for a staircase modulation

The goal is to find optimal switching angles that minimize voltage (current) waveform Mean Square approximation error (2). In fact, that will deliver minimal THD (1) accounting for all switching harmonics due to Parseval theorem (Rayleigh energy theorem) -

$$THD(m),\% = \frac{\sqrt{2NMS(m)}}{m} \cdot 100 \quad [\%]. \tag{3}$$

This way, THD minimization problem is formulated in time domain as constrained optimization one.

NMS (2) is the target function to be minimized. For instance, for the Fig.1 waveform it becomes

$$NMS(m,\alpha_1,\alpha_2) = 1 - \frac{1}{2}m^2 - \frac{2}{4\pi}(\alpha_1 + 3\alpha_2). \tag{4}$$

There are also equality and inequality constraints. The equality constraint is due to fundamental voltage harmonic (modulation index *m)* requirement by the fundamental Fourier series term

$$m = \frac{2}{\pi}[\cos(\alpha_1) + \cos(\alpha_2)]. \tag{5}$$

Additionally, there are staircase modulation switching angles limitations –

$$0 < \alpha_1 < \sin^{-1}[1/(2m)]; \quad \sin^{-1}[1/(2m)] < \alpha_2 < \pi/2. \tag{6}$$

The formulas for NMS, modulation index, and switching angles (4)-(6) may be easily extended for an arbitrary level / switching angles count [12].

Current THD time domain analysis challenge in the pure inductive load approximation (WTHD) is finding closed-form expressions for current approximation mean square error for piece-wise linear current waveforms obtained by time integration of staircase voltage waveforms (Fig.2).

Current ripple NMS expressions under the assumption of

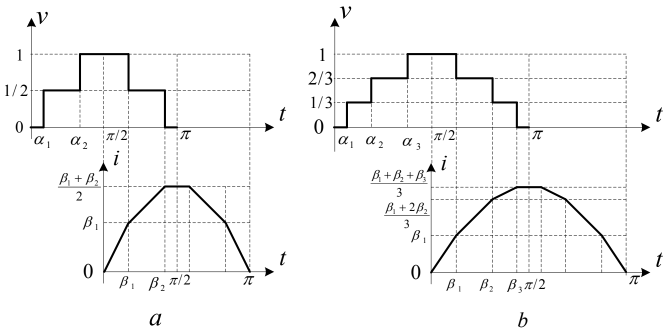

Fig. 2. Piece-wise linear current waveform approximation examples for three- (a) and four-level (b) inverters

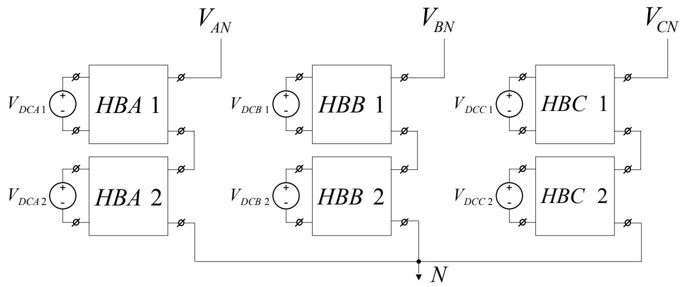

Fig. 3. Three-phase cascade inverter topology

pure inductive load are derived in [12] based on formula (2) for an arbitrary level / switching angle count. For instance, most simple expression for a three-level two angle inverter (Fig.2,a)

$$NMS(m,\beta_1,\beta_2) = \frac{(\beta_1+\beta_2)^2}{4} - \frac{\frac{\beta_1^3}{2} + \frac{\beta_1\beta_2^3}{2} + \frac{\beta_2^3}{3}}{\pi} - \frac{1}{2}m^2; \tag{7}$$

$$\beta_1 = \pi/2 - \alpha_2, \quad \beta_2 = \pi/2 - \alpha_1.$$

The constrained NMS (THD) optimization problems with modulation index equality and switching angles inequalities are effectively solved by means of Matlab function *fmicon*. The examples of single-phase inverter minimal voltage and current THD and optimal switching angles solutions are given in [12].

III. Three-Phase Cascaded Inverter Minimal Voltage and Current THD Time Domain Problem Formulation

A three-phase cascaded inverter topology with two H-bridges per phase is shown in Fig.3. The analysis in this paper assumes equal voltages of all DC sources (uniformly distributed voltage levels).

Minimization of a balanced load THD requires considering the line-to-line inverter voltages [14]. When addressing current THD, delta load connection is assumed (the results will be applicable to star-connected load as well).

Consider first relatively small modulation indices meaning two-level single switching angle voltage waveforms in each phase. Though there is no room for optimization because there is only one degree of freedom, it is instructive and assists in better understanding the peculiarities of the three-phase case.

There are three different situations listed below to consider in the modulation index increase order:

Case 1. $\pi/3 < \alpha < \pi/2$

Case 2. $\pi/6 < \alpha < \pi/3$

Case 3. $0 < \alpha < \pi/6$

Phase and line-to-line voltage waveforms for the three cases are given in Fig.4, 5, 6 respectively. Note that in the line-to-line voltages there are two switching angles.

For the smallest modulation indices / large angles (Case 1), line-to-line voltage waveform (Fig.4) differs from the staircase shape with the switching angles

$$\begin{aligned} \beta_1 &= \alpha - \pi/6; \\ \beta_2 &= 5\pi/6 - \alpha. \end{aligned} \tag{8}$$

For the Case 2 and 3, the line-to-line voltage waveform is staircase (Fig.5, 6). However, the line-to-line switching angles dependences on the phase switching angle are different being

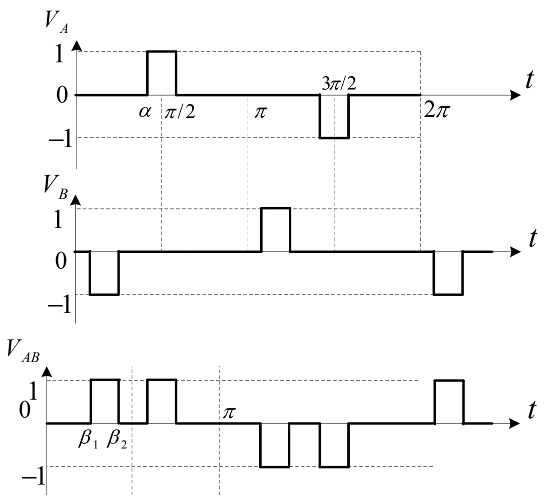

Fig. 4. Phase and line-to-line voltages for Case 1

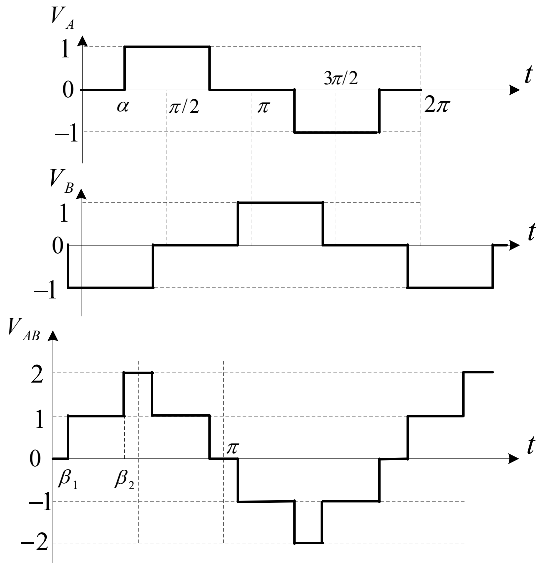

Fig. 5. Phase and line-to-line voltages for Case 2

$$\beta_1 = \alpha - \pi/6; \quad \beta_2 = \alpha + \pi/6 \tag{9}$$

and

$$\beta_1 = \pi/6 - \alpha; \quad \beta_2 = \pi/6 + \alpha. \tag{10}$$

It is easy to calculate modulation index and voltage ripple NMS for the three cases as a function of phase switching angle. For instance, for Case 3 (Fig.6) accounting for (10) modulation index becomes

$$m = \frac{4}{\pi}\left(\cos\beta_1 + \cos\beta_2\right) = \frac{4\sqrt{3}}{\pi}\cos\alpha. \tag{11}$$

Note that it is about the line-to-line modulation index that for the cascaded H-bridge inverter of Fig.3 reaches 4 and more for line-to-line staircase waveforms with five levels / four angles.

Using (2), (10), and (11), voltage ripple NMS for Case 3 is found as

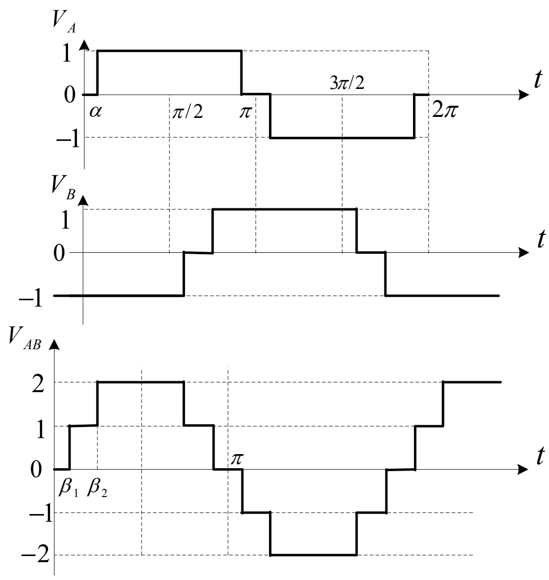

Fig. 6. Phase and line-to-line voltages for Case 3

$$NMS = \overline{V_{AB}^2} - \frac{m^2}{2} = \frac{2}{\pi}\left[1\cdot(\beta_2-\beta_1) + 4\cdot\left(\frac{\pi}{2}-\beta_2\right)\right] - \frac{m^2}{2} = \frac{8}{3} - \frac{4\alpha}{\pi} - \frac{24}{\pi^2}\cos^2\alpha. \tag{12}$$

For two phase switching angles, there are nine distinct modulation regions shown in Fig.7 ([16], [17]) with four line-to-line switching angles. The regions differ in phase switching angle limitations, line-to-line switching angles expressions and voltage and current waveform shapes (see Appendix).

There are four different types of line-to-line voltage and current waveform shapes shown in Appendix (regions 1; 2; 3, 5, 6; 4, 7, 8, 9). Voltage and current ripple NMS formulas for every region are found by calculating waveform mean squares according to formula (2). For example, for regions 4, 7, 8, 9, the waveforms are similar to those for single-phase staircase modulation and voltage and current NMS become ([12])

$$NMS_V = 16 - \frac{1}{2}m^2 - \frac{2}{\pi}\left(\beta_1 + 3\beta_2 + 5\beta_3 + 7\beta_4\right); \tag{13}$$

$$NMS_I = (\beta_1+\beta_2+\beta_3+\beta_4)^2 - \frac{1}{3\pi}(10\beta_1^3 + 6\beta_1\beta_2^2 + 6\beta_1\beta_3^2 + 6\beta_1\beta_4^2 + 8\beta_2^3 + 6\beta_2\beta_3^2 + 6\beta_2\beta_4^2 + 6\beta_3^3 + 6\beta_3\beta_4^2 + 4\beta_4^3) - \frac{1}{2}m^2, \tag{14}$$

where line-to-line modulation index

$$m = \frac{4}{\pi}[\cos(\beta_1) + \cos(\beta_2) + \cos(\beta_3) + \cos(\beta_4)]. \tag{15}$$

Once NMS and modulation index formulas for every region are found, it is possible to perform local (per region) NMS (THD) minimization and based on local results the global one. The local NMS minimization problem is formulated as constrained optimization one with NMS as a target function, modulation index equation (15) as equality constraint and phase angle limitations (Appendix) as inequality constraints.

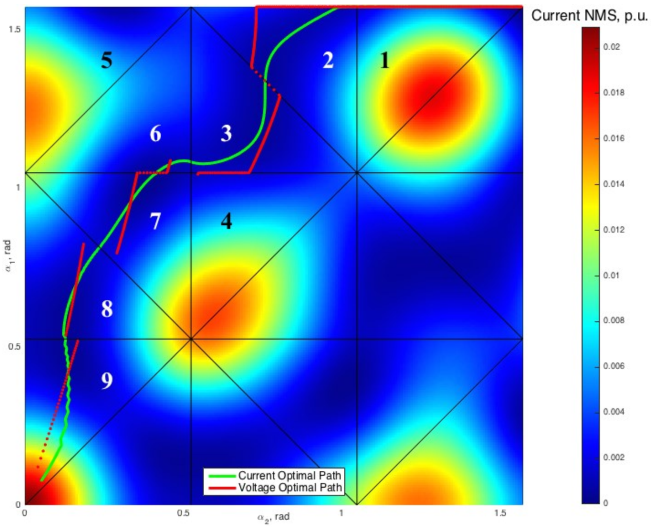

Fig. 7. Modulation regions and voltage and current optimal angle paths

Matlab *fmincon* function is an adequate solver for local constrained optimization problems that delivers a solution for a given modulation index within a fraction of second.

The results of voltage and current quality optimization are presented and discussed in the next Section.

IV. Three-Phase Cascaded Inverter Voltage and Current THD Minimization Results

Voltage and current quality optimization is performed for the whole modulation index range. Voltage and current optimal phase switching angle paths are presented in Fig.7.

Voltage and current optimal angles dependence on modulation index is shown in Fig.8. It is observed that voltage optimal switching angles trajectories are not smooth and have discontinuities [16] as opposed to the current optimal ones.

Optimal voltage THD for a three-phase cascaded inverter is given in Fig.9 in comparison with that for a single-phase inverter with staircase modulation with four cascaded H-bridges (Fig.10). In general, the single-phase voltage quality is better and this is because for the staircase three-phase line-to-line waveforms there are less degrees of freedom - two vs four ones for a single-phase inverter. Non-staircase three-phase line-to-line voltage waveforms (regions 2, 3, 5, 6) are disadvantageous from voltage quality perspective. There are seven points where the three-phase THD curve touches the single-phase one that means equal voltage THD for respective modulation indices.

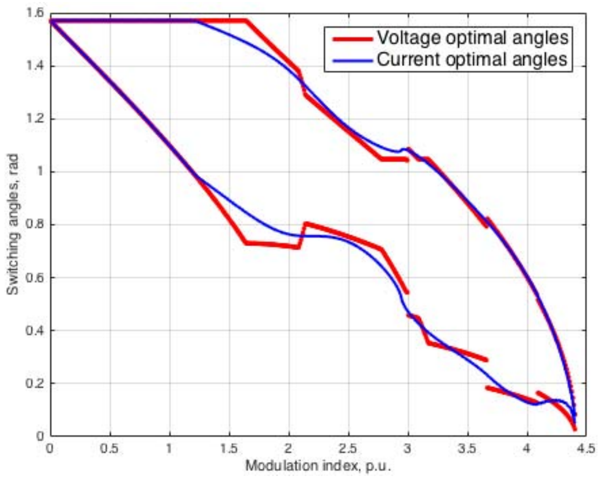

Fig. 8. Voltage and current optimal phase switching angles

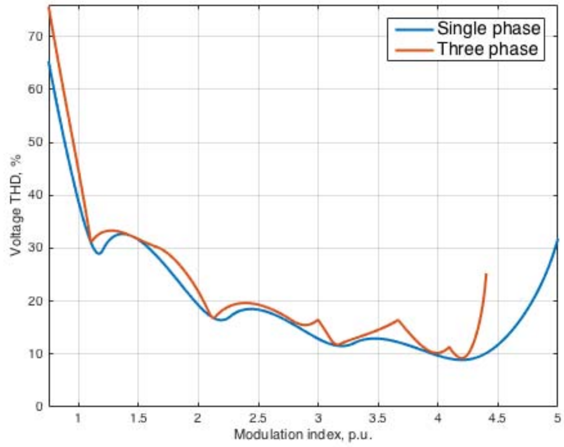

Fig. 9. Comparison of minimal voltage THD for three-phase cascade and single-phase inverters

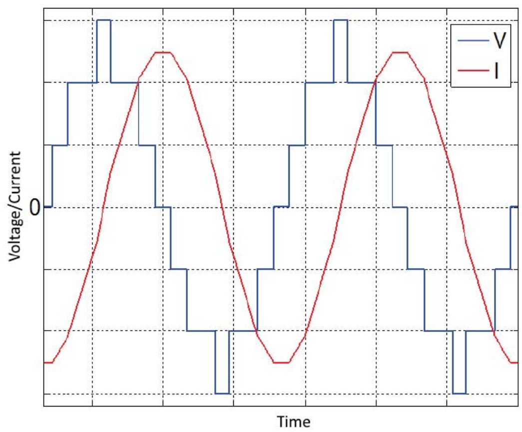

Fig. 10. An example of a staircase modulation for four-level single-phase inverter – current waveform is obtained by voltage waveform integration

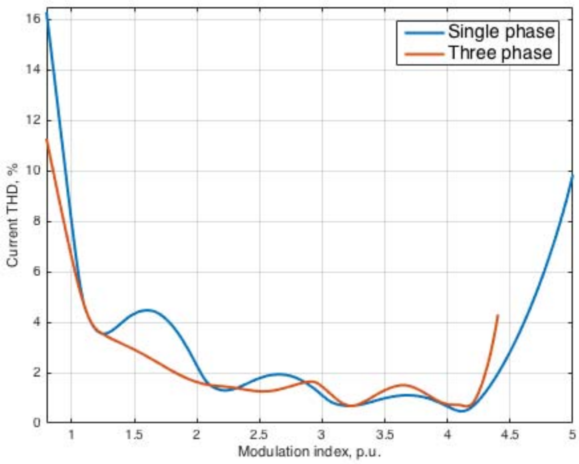

Fig. 11. Comparison of minimal current THD for three-phase cascade and single-phase inverters

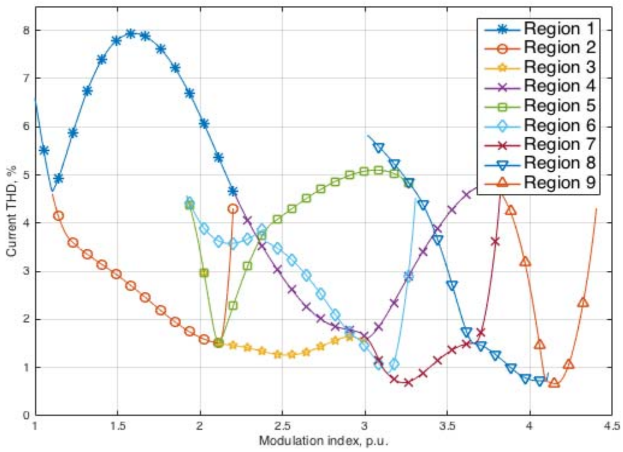

Fig. 12. Global current THD optimization

Optimal current THD for a three-phase cascaded inverter is compared with that for a single-phase one in Fig.11.

For relatively large modulation indices, single-phase current quality is better because for staircase three-phase line-to-line waveforms there are less degrees of freedom - two vs four ones for a single-phase inverter. The upper three-phase THD curve touches the lower single-phase one in three points (Fig.11).

It is interesting and this may come as a surprise that, for relatively small modulation indices, three-phase cascaded inverter current quality is better. The reason is that line-to-line voltage waveforms (regions 2, 3, 5, 6) are non-staircase meaning that they have increased amount of switching compared with their single-phase staircase counterparts. While this is disadvantageous from the voltage quality perspective (Fig.9), it is beneficial from the current quality one (Fig.11).

Fig.12 gives an idea how the optimal current THD graph is obtained as the result of global optimization. The nine THD curves present the results of local optimization within nine respective regions.

V. Conclusions

The paper presents the results of voltage and current quality optimization for a three-phase cascaded H-bridge inverter with a fundamental phase staircase modulation. THD minimization problems are formulated in time domain as constraint optimization ones accounting for all switching harmonics.

Optimal voltage THD results practically coincide with those reported in [17]. However, the authors of [17] account for all switching harmonics by finding closed form expressions for infinite sums that appear in THD frequency domain definition. By applying the time domain analysis, this extra effort is totally eliminated that allows focusing on the physical essence of the problem. Comparison of voltage quality of a three-phase cascaded inverter and its single-phase counterpart with a staircase modulation shows that it is better for a single-phase inverter. Three-phase cascaded inverter current optimal switching angles and minimal current THD are systematically presented for the first time.

For relatively small modulation indices, three-phase cascaded inverter current quality is better than that of a single-phase counterpart with a staircase modulation. This is because the line-to-line voltage waveforms are non-staircase and have increased amount of switching compared with their single-phase staircase counterparts that is disadvantageous for voltage quality but beneficial from the current quality perspective.

Voltage and current THD minimization results (Fig. 9, 11) are fully supported by PSIM simulations for inductance dominated loads with optimal switching angles (Fig.8).

References

[1] J. Rodriguez, S. Bernet, Bin Wu, J.O. Pontt, and S. Kouro, "Multilevel voltage-source-converter topologies for industrial medium-voltage drives," *IEEE Trans. Ind. Electron.*, vol. 54, no. 6, pp. 2930–2945, Dec. 2007.

[2] G. Buticchi, D. Barater, E. Lorenzani, C. Concari, and G. Franceschini, "A nine-level grid-connected converter topology for single-phase transformerless PV systems," *IEEE Trans. Ind. Electron.*, vol. 61, no. 8, pp. 3951–3960, Aug. 2014.

[3] A. Mora, P. Lezana, and J. Juliet, "Control scheme for an induction motor fed by a cascaded multicell converter under internal fault," *IEEE Trans. Ind. Electron.*, vol. 61, no. 11, pp. 5948–5955, Nov. 2014.

[4] A. Ruderman, B. Reznikov, and S. Busquets-Monge, "Asymptotic time domain evaluation of a multilevel multiphase PWM converter voltage quality," *IEEE Trans. Ind. Electron.*, vol. 60, no. 5, pp. 1999–2009, May 2013.

[5] B. Reznikov, M. Srndovic, Y. Familiant, G. Grandi, and A. Ruderman, "Simple Time Averaging Current Quality Evaluation of a Single-Phase Multilevel PWM Inverter," accepted for publication in *IEEE Trans. Ind. Electron.*, 2016.

[6] H.W. van der Broeck, H.-C. Skudelny, and G.V. Stanke, "Analysis and realization of a pulsewidth modulator based on state space vectors," *IEEE Trans. Ind. Appl.,* vol. 24, no. 1, part 1, pp. 142-150, Jan.-Feb. 1988.

[7] M. S. A. Dahidah, G. Konstantinou, and V.G. Agelidis, "A review of multilevel selective harmonic elimination PWM: formulations, solving algorithms, implementation and applications," IEEE Trans. Power Electron., vol. 30, no. 8, pp. 4091–4106, Aug. 2015.

[8] IEEE Recommended Practices and Requirements for Harmonic Control in Electrical Power Systems," *IEEE Std 519-1992*, pp.1-112, April 9, 1993.

[9] C.A.L. Espinosa, I. Portocarrero, and M. Izquierdo, "Minimization of THD and angles calculation for multilevel inverters," *Int. Journal of Eng. and Technology IJET-IJENS*, vol. 12, no. 5, pp. 83-86, Oct. 2012.

[10] Fang Lin Luo, "Investigation on best switching angles to obtain lowest THD for multilevel DC/AC inverters," *Proc. Int. 8th IEEE Conf. on Ind. Electron. and Appl.*, June 2013, pp.1814-1818.

[11] E.E. Espinosa, J.R. Espinoza, P.E. Melin, R.O. Ramirez, F. Villarroel, J.A. Munoz, and L. Moran, "A new modulation method for a 13-level asymmetric inverter toward minimum THD," *IEEE Trans. Ind. Appl.*, vol. 50, no. 3, pp. 1924–1933, May-June 2014.

[12] K. Koishybay, Y.L. Familiant, and A. Ruderman,"Minimization of voltage and current total harmonic distortion for a single-phase multilevel inverter staircase modulation," *Proc. 9th Int. Conf. on Power Electronics (ICPE – ECCE Asia)*, June 2015, pp. 1203-1208.

[13] Y. Liu, H. Hong, and A. Huang, "Real-time calculation of switching angles minimizing THD for multilevel inverters with step modulation," *IEEE Trans. Ind. Electron.*, vol. 56, no. 2, pp. 285–293, Feb. 2009.

[14] N. Yousefpoor, S. Fathi, N. Farokhnia, and H. Abyaneh, "THD minimization applied directly on the line-to-line voltage of multilevel inverters," *IEEE Trans. Ind. Electron.*, vol. 59, no. 1, pp. 373–380, Jan. 2012.

[15] B. Diong, H. Sepahvand, and K.A. Corzine, "Harmonic distortion optimization of cascaded H-bridge inverters considering device voltage drops and noninteger DC voltage ratios," *IEEE Trans. Ind. Electron.*, vol. 60, no. 8, pp. 3106–3114, Aug. 2013.

[16] R. Fotouhi, A. Sorokin, R. Kennel, and H. du Toit Mouton, "An efficient method to calculate optimal pulse patterns for multi-level converters," *Proc. 9th Int. Conf. on Power Electronics (ICPE – ECCE Asia)*, June 2015, pp. 533-539.

[17] D. Hong, S. Bai, and S.M. Lukic, "Closed-form expressions for minimizing total harmonic distortion in three-phase multilevel converters," IEEE Trans. Power Electron., vol. 29, no. 10, pp. 5229–5241, Oct. 2014.

Region	Boundary conditions	Voltage line angles	Current line angles	Waveform
1	$\frac{\pi}{3}<\alpha_1<\frac{\pi}{2}$ $\frac{\pi}{3}<\alpha_2<\frac{\pi}{2}$ $\alpha_1<\alpha_2$ $0<M$ $M<0.551$	$\beta_1=\alpha_1-\frac{\pi}{6}$ $\beta_2=\alpha_2-\frac{\pi}{6}$ $\beta_3=\frac{5\pi}{6}-\alpha_2$ $\beta_4=\frac{5\pi}{6}-\alpha_1$	$\beta_1=\alpha_1-\frac{\pi}{3}$ $\beta_2=\alpha_2-\frac{\pi}{3}$ $\beta_3=\frac{2\pi}{3}-\alpha_2$ $\beta_4=\frac{2\pi}{3}-\alpha_1$	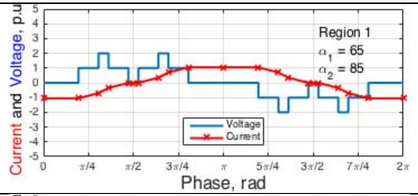
2	$\frac{\pi}{6}<\alpha_1<\frac{\pi}{3}$ $\frac{\pi}{3}<\alpha_2<\frac{\pi}{2}$ $\alpha_1+\alpha_2>\frac{2\pi}{3}$ $0.276<M$ $M<0.551$	$\beta_1=\alpha_1-\frac{\pi}{6}$ $\beta_2=\alpha_2-\frac{\pi}{6}$ $\beta_3=\frac{5\pi}{6}-\alpha_2$ $\beta_4=\alpha_1+\frac{\pi}{6}$	$\beta_1=\frac{\pi}{3}-\alpha_1$ $\beta_2=\alpha_2-\frac{\pi}{3}$ $\beta_3=\frac{2\pi}{3}-\alpha_2$ $\beta_4=\frac{2\pi}{3}-\alpha_1$	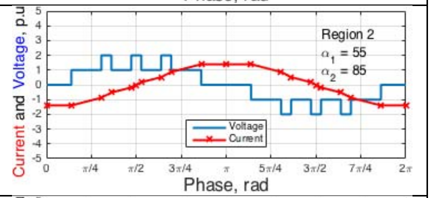
3	$\frac{\pi}{6}<\alpha_1<\frac{\pi}{3}$ $\frac{\pi}{3}<\alpha_2<\frac{\pi}{2}$ $\alpha_1+\alpha_2<\frac{2\pi}{3}$ $0.478<M$ $M<0.753$	$\beta_1=\alpha_1-\frac{\pi}{6}$ $\beta_2=\alpha_2-\frac{\pi}{6}$ $\beta_3=\alpha_1+\frac{\pi}{6}$ $\beta_4=\frac{5\pi}{6}-\alpha_2$	$\beta_1=\alpha_2-\frac{\pi}{3}$ $\beta_2=\frac{\pi}{3}-\alpha_1$ $\beta_3=\frac{2\pi}{3}-\alpha_2$ $\beta_4=\frac{2\pi}{3}-\alpha_1$	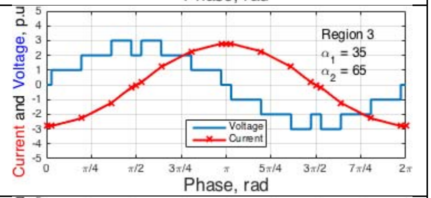
4	$\frac{\pi}{6}<\alpha_1<\frac{\pi}{3}$ $\frac{\pi}{6}<\alpha_2<\frac{\pi}{3}$ $\alpha_1<\alpha_2$ $0.551<M$ $M<0.955$	$\beta_1=\alpha_1-\frac{\pi}{6}$ $\beta_2=\alpha_2-\frac{\pi}{6}$ $\beta_3=\alpha_1+\frac{\pi}{6}$ $\beta_4=\alpha_2+\frac{\pi}{6}$	$\beta_1=\frac{\pi}{3}-\alpha_2$ $\beta_2=\frac{\pi}{3}-\alpha_1$ $\beta_3=\frac{2\pi}{3}-\alpha_2$ $\beta_4=\frac{2\pi}{3}-\alpha_1$	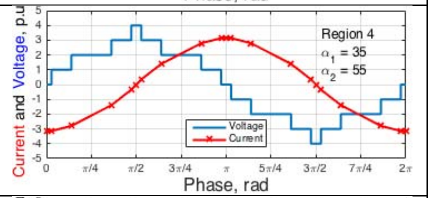
5	$0<\alpha_1<\frac{\pi}{6}$ $\frac{\pi}{3}<\alpha_2<\frac{\pi}{2}$ $\alpha_2-\alpha_1>\frac{\pi}{3}$ $0.478<M$ $M<0.827$	$\beta_1=\frac{\pi}{6}-\alpha_1$ $\beta_2=\alpha_1+\frac{\pi}{6}$ $\beta_3=\alpha_2-\frac{\pi}{6}$ $\beta_4=\frac{5\pi}{6}-\alpha_2$	$\beta_1=\alpha_2-\frac{\pi}{3}$ $\beta_2=\frac{2\pi}{3}-\alpha_2$ $\beta_3=\frac{\pi}{3}-\alpha_1$ $\beta_4=\frac{\pi}{3}+\alpha_1$	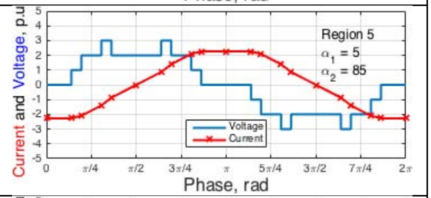
6	$0<\alpha_1<\frac{\pi}{6}$ $\frac{\pi}{3}<\alpha_2<\frac{\pi}{2}$ $\alpha_2-\alpha_1<\frac{\pi}{3}$ $0.478<M$ $M<0.827$	$\beta_1=\frac{\pi}{6}-\alpha_1$ $\beta_2=\alpha_2-\frac{\pi}{6}$ $\beta_3=\alpha_1+\frac{\pi}{6}$ $\beta_4=\frac{5\pi}{6}-\alpha_2$	$\beta_1=\alpha_2-\frac{\pi}{3}$ $\beta_2=\frac{\pi}{3}-\alpha_1$ $\beta_3=\frac{2\pi}{3}-\alpha_2$ $\beta_4=\frac{\pi}{3}+\alpha_1$	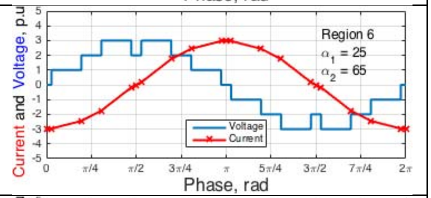
7	$0<\alpha_1<\frac{\pi}{6}$ $\frac{\pi}{6}<\alpha_2<\frac{\pi}{3}$ $\alpha_1+\alpha_2>\frac{\pi}{3}$ $0.753<M$ $M<0.955$	$\beta_1=\frac{\pi}{6}-\alpha_1$ $\beta_2=\alpha_2-\frac{\pi}{6}$ $\beta_3=\alpha_1+\frac{\pi}{6}$ $\beta_4=\alpha_2+\frac{\pi}{6}$	$\beta_1=\frac{\pi}{3}-\alpha_2$ $\beta_2=\frac{\pi}{3}-\alpha_1$ $\beta_3=\frac{2\pi}{3}-\alpha_2$ $\beta_4=\frac{\pi}{3}+\alpha_1$	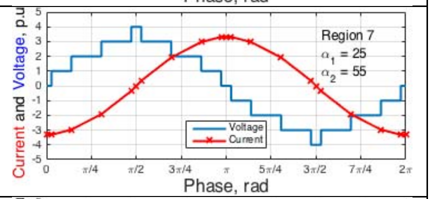
8	$0<\alpha_1<\frac{\pi}{6}$ $\frac{\pi}{6}<\alpha_2<\frac{\pi}{3}$ $\alpha_1+\alpha_2<\frac{\pi}{3}$ $0.827<M$ $M<1.029$	$\beta_1=\alpha_2-\frac{\pi}{6}$ $\beta_2=\frac{\pi}{6}-\alpha_1$ $\beta_3=\alpha_1+\frac{\pi}{6}$ $\beta_4=\alpha_2+\frac{\pi}{6}$	$\beta_1=\frac{\pi}{3}-\alpha_2$ $\beta_2=\frac{\pi}{3}-\alpha_1$ $\beta_3=\frac{\pi}{3}+\alpha_1$ $\beta_4=\frac{2\pi}{3}-\alpha_2$	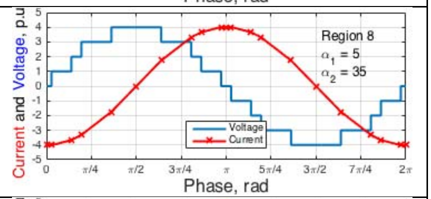
9	$0<\alpha_1<\frac{\pi}{6}$ $0<\alpha_2<\frac{\pi}{6}$ $\alpha_1<\alpha_2$ $0.955<M$ $M<1.103$	$\beta_1=\frac{\pi}{6}-\alpha_2$ $\beta_2=\frac{\pi}{6}-\alpha_1$ $\beta_3=\alpha_1+\frac{\pi}{6}$ $\beta_4=\alpha_2+\frac{\pi}{6}$	$\beta_1=\frac{\pi}{3}-\alpha_2$ $\beta_2=\frac{\pi}{3}-\alpha_1$ $\beta_3=\frac{\pi}{3}+\alpha_1$ $\beta_4=\frac{\pi}{3}+\alpha_2$	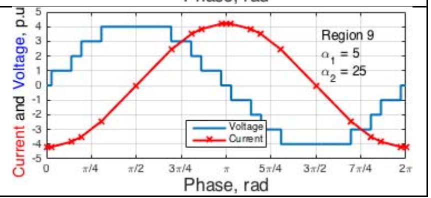

APPENDIX. Different modulation regions with phase angle limitations, voltage and current line-to-line angles expressions (counted from increasing fundamental harmonic zero) and representative waveforms